

REPORT DOCUMENTATION PAGE					Form Approved OMB No. 0704-01-0188	
The public reporting burden for this collection of information is estimated to average 1 hour per response, including the time for reviewing instructions, searching existing data sources, gathering and maintaining the data needed, and completing and reviewing the collection of information. Send comments regarding this burden estimate or any other aspect of this collection of information, including suggestions for reducing the burden to Department of Defense, Washington Headquarters Services, Directorate for Information Operations and Reports (0704-0188), 1215 Jefferson Davis Highway, Suite 1204, Arlington VA 22202-4302. Respondents should be aware that notwithstanding any other provision of law, no person shall be subject to any penalty for failing to comply with a collection of information if it does not display a currently valid OMB control number.						
PLEASE DO NOT RETURN YOUR FORM TO THE ABOVE ADDRESS.						
1. REPORT DATE (DD-MM-YYYY) 08-10-2005		2. REPORT TYPE REPRINT		3. DATES COVERED (From - To)		
4. TITLE AND SUBTITLE Reactions of N^+ , N_2^+ , and N_3^+ with NO from 300 to 1400 K				5a. CONTRACT NUMBER		
				5b. GRANT NUMBER		
				5c. PROGRAM ELEMENT NUMBER 61102F		
6. AUTHORS Anthony J. Midey, Thomas M. Miller and A.A. Viggiano				5d. PROJECT NUMBER 2303		
				5e. TASK NUMBER BM		
				5f. WORK UNIT NUMBER A1		
7. PERFORMING ORGANIZATION NAME(S) AND ADDRESS(ES) Air Force Research Laboratory /VSBXT 29 Randolph Road Hanscom AFB, MA 01731-3010				8. PERFORMING ORGANIZATION REPORT NUMBER AFRL-VS-HA-TR-2005-1188		
9. SPONSORING/MONITORING AGENCY NAME(S) AND ADDRESS(ES)				10. SPONSOR/MONITOR'S ACRONYM(S) AFRL/VSBXT		
				11. SPONSOR/MONITOR'S REPORT NUMBER(S)		
12. DISTRIBUTION/AVAILABILITY STATEMENT Approved for public release; distribution unlimited.						
13. SUPPLEMENTARY NOTES Reprinted from J. Chem. Phys., Vol. 121, No. 14. (2004)						
14. ABSTRACT Rate constants have been measured from 300 to 1400 K in a selected ion flow tube and a high temperature flowing afterglow for the reactions of N^+ , N_2^+ , and N_3^+ with NO. In all of the systems, the rate constants are substantially less than the collision rate constant. Comparing the high temperature results to kinetics studies as a function of translational energy show that all types of energy (translational, rotational, and vibrational) affect the reactivity approximately equally for all three ions. Branching ratios have also been measured at 300 and 5000 K in a selected ion flow tube for the N^+ and N_3^+ reactions. An increase in the N_2^+ product at the expense of NO^+ nondissociative charge transfer product occurs at 500 K with N^+ . The branching ratios for the reaction of N_3^+ with NO have also been measured in the selected ion flow tube, showing that only nondissociative charge transfer giving NO^+ occurs up to 500 k. The current results are discussed in the context of the many previous studies of these ions in the literature.						
15. SUBJECT TERMS Rate constants Temperature dependence Nitric oxide High temperature						
16. SECURITY CLASSIFICATION OF:			17. LIMITATION OF ABSTRACT	18. NUMBER OF PAGES	19a. NAME OF RESPONSIBLE PERSON	
a. REPORT	b. ABSTRACT	c. THIS PAGE			A. A. Viggiano	
UNCL	UNCL	UNCL	UNL		19b. TELEPHONE NUMBER (Include area code) (781) 377-4028	

Reactions of N^+ , N_2^+ , and N_3^+ with NO from 300 to 1400 K

Anthony J. Midey,^{a)} Thomas M. Miller, and A. A. Viggiano

Air Force Research Laboratory, Space Vehicles Directorate, Hanscom Air Force Base, Massachusetts 01731-3010

(Received 23 June 2004; accepted 21 July 2004)

Rate constants have been measured from 300 to 1400 K in a selected ion flow tube (SIFT) and a high temperature flowing afterglow for the reactions of N^+ , N_2^+ and N_3^+ with NO. In all of the systems, the rate constants are substantially less than the collision rate constant. Comparing the high temperature results to kinetics studies as a function of translational energy show that all types of energy (translational, rotational, and vibrational) affect the reactivity approximately equally for all three ions. Branching ratios have also been measured at 300 and 500 K in a SIFT for the N^+ and N_3^+ reactions. An increase in the N_2^+ product at the expense of NO^+ nondissociative charge transfer product occurs at 500 K with N^+ . The branching ratios for the reaction of N_3^+ with NO have also been measured in the SIFT, showing that only nondissociative charge transfer giving NO^+ occurs up to 500 K. The current results are discussed in the context of the many previous studies of these ions in the literature. [DOI: 10.1063/1.1792232]

I. INTRODUCTION

Measurements of the kinetics of ion-molecule reactions at high temperatures have proven that the internal energy available at these elevated temperatures can have a significant effect on the rate constants and product branching ratios.¹ These data show that extrapolations to high temperature behavior based solely on room temperature data could be seriously in error. The results have been invaluable in modeling the chemistry at elevated temperatures involving plasmas.^{2,3}

The reactivities of the nitrogen ion species N_m^+ where $m=1-3$ are of particular interest. Both N^+ and N_2^+ are key precursor ions in the complex chemistry of the ionosphere⁴⁻⁶ and N_3^+ ions are readily formed in rf discharges.⁷⁻⁹ In addition, NO^+ ions are one of the main terminal ions in air plasma environments and are a major component of the daytime ionosphere of altitude of 200 km,⁵ making reactions with NO especially interesting.

Considering the importance of the ion-molecule chemistry of nitrogen cations with NO, the rate constants for the reactions of N^+ , N_2^+ , and N_3^+ with NO have been studied up to 1400 K using a selected ion flow tube (SIFT) and a high temperature flowing afterglow (HTFA). Previous drift tube studies of the kinetics as a function of reactant translational energy have been done at 298 K for all three ions.¹⁰⁻¹⁵ Thus, comparing the current results with the drift tube data illustrates the effects of internal energy on the reactivity. In addition, the temperature dependence of the branching ratios for the reactions of N^+ and N_3^+ have been measured up to 500 K in the SIFT where the reactant ions are mass selected. The products for the N^+ reaction have previously been measured only at 298 K,¹⁶⁻¹⁸ indicating that another reactive channel occurs in addition to charge transfer. However, the

product branching ratios for the N_3^+ reaction have not been measured previously. For each individual ion-molecule reaction, numerous previous studies using several different methods will be discussed to better understand the current results.

II. EXPERIMENT

Rate constants for the N^+ , N_2^+ , and N_3^+ reactions with NO have been measured using both a SIFT and HTFA at the Air Force Research Laboratory. The instruments have been described in detail elsewhere,^{19,20} including later modifications to the upstream ion source region of the HTFA.²¹ The helium buffer gas was passed through a liquid nitrogen cooled sieve trap to remove water vapor. The NO was also passed through a sieve trap to reduce the minute amount of impurities in the sample. In the following sections, only the details pertinent to the current experiments will be discussed.

In the SIFT, electron impact on nitrogen gas taken from the boiloff of a high pressure liquid nitrogen dewar and introduced into an effusive source produced N^+ ions in a high pressure source chamber. N_3^+ ions were simultaneously generated by the three-body reaction of N^+ with N_2 and Penning ionization of N_2 with N_2^+ in the source. The ion of interest was mass selected with a quadrupole mass analyzer and injected into a fast flow of helium buffer gas (AGA, 99.997%) that was introduced through a Venturi inlet. These ions became thermally equilibrated before entering the reaction zone where NO gas (AGA, 99.8%) was added.

After reaction over a known distance at a previously measured reaction time under pseudo-first-order conditions, the remaining ions were sampled through an aperture in a blunt nose cone, mass analyzed, and then detected. The product distribution was determined by extrapolating the branching ratios to zero NO flow to minimize the effects of secondary reactions with NO in the flow tube, leading to relative

^{a)}Author to whom correspondence should be addressed. Electronic mail: anthony.midey@hanscom.af.mil

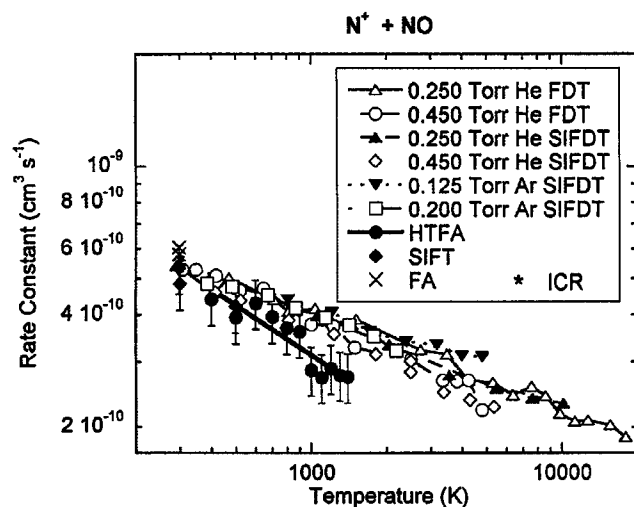


FIG. 1. Rate constants for the reaction of N^+ with NO plotted as a function of temperature. The flow drift tube (FDT) and selected ion flow drift tube (SIFDT) data are from Fahey *et al.* (Ref. 12). The high temperature flowing afterglow (HTFA) data are current measurements. The selected ion flow tube (SIFT) data represent previous measurements at 298 K by Adams *et al.* (Ref. 18) and Tichy *et al.* (Ref. 17), as well as the current SIFT measurements at 300 and 500 K. The flowing afterglow (FA) value is from Matsuoka *et al.* (Ref. 26) and the ion cyclotron resonance mass spectrometer (ICR) value is from Anicich *et al.* (Ref. 16).

errors in the branching ratios of $\pm 10\%$ of the major product peaks.²² The experimental rate constants have relative uncertainties of $\pm 15\%$ and absolute uncertainties of $\pm 25\%$.¹⁹

In the HTFA, the three nitrogen cations of interest were generated simultaneously without mass selection in an ion source region upstream of and perpendicular to the main flow tube. The helium buffer flow was introduced into the source region through an inlet behind a thoriated iridium filament. Electron impact on the buffer gas generated He^* and He^+ ions. These ions reacted with nitrogen gas introduced downstream from the filament to generate N^+ and N_2^+ ions. The N_3^+ ions were generated through the same two mechanisms as in the SIFT. The pressure in the source region was increased by the use of a 0.25 in. diameter diaphragm so that the N_2 concentration in the flow tube was low enough to minimize the clustering reaction there. The various ions were transported into the flow tube by the fast flow of buffer gas where a commercially available furnace heated the flow tube to the desired temperature. These ions became thermally equilibrated before entering the reaction zone where the NO was introduced. Again, after reaction over a known distance at a previously measured reaction time under pseudo-first-order conditions, the remaining ions were sampled through an aperture in a blunt nose cone, mass analyzed, and then detected. The experimental rate constants measured with the HTFA have relative uncertainties of $\pm 15\%$ and absolute uncertainties of $\pm 25\%$.²⁰

III. RESULTS

A. $N^+ + NO$

The reaction of N^+ with NO has been extensively studied in the past.^{11,12,16–18,23–27} Rate constants for this reaction are shown in Fig. 1 plotted against temperature. For the drift

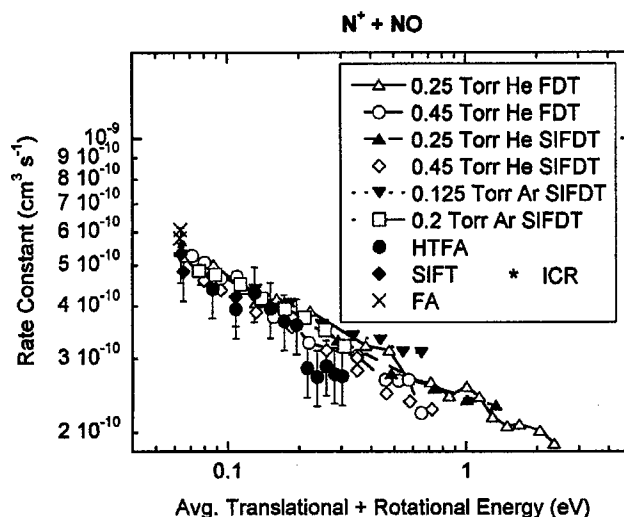


FIG. 2. Rate constants for the reaction of N^+ with NO plotted as a function of the average translational and rotational energy in eV. The FDT and SIFDT data are from Fahey *et al.* (Ref. 12). The HTFA data are current measurements. The SIFT data represent previous measurements at 298 K by Adams, Smith, and Paulson (Ref. 18) and Tichy *et al.* (Ref. 17) as well as the current SIFT measurements at 300 and 500 K. The FA value is from Matsuoka *et al.* (Ref. 26) and the ICR value is from Anicich *et al.* (Ref. 16).

tube data measured in a flow drift tube (FDT) and selected-ion flow drift tube (SIFDT),¹² the center-of-mass kinetic energies have been converted to an effective translational temperature T_{eff} , where $T_{\text{eff}} = 2\langle KE_{\text{c.m.}} \rangle / 3k_B T$ and k_B is Boltzmann's constant. The rate constants decrease with increasing temperature and can be represented by a power law as $(6.5 \times 10^{-9})T^{-0.44}$. The room temperature rate constants shown in Fig. 1 measured in various fast flow tube instruments^{12,17,18,26} as well as an ion cyclotron resonance (ICR) mass spectrometer¹⁶ are in good agreement, having a value of $ca. 5.5 \pm 0.7 \times 10^{-10} \text{ cm}^3 \text{ s}^{-1}$. Two measurements of the rate constant are not shown in Fig. 1 because they were made in the early days of the flowing afterglow, before error levels had been reduced. Those measurements gave somewhat larger values of $8\text{--}9 \times 10^{-10} \text{ cm}^3 \text{ s}^{-1}$.^{23,24} The average value of the room temperature rate constant is approximately one-half of the Su-Chesnavich collision rate constant^{28,29} of $1.0 \times 10^{-9} \text{ cm}^3 \text{ s}^{-1}$. The new SIFT and HTFA data are in agreement with the drift tube data¹² up to 900 K within the 15% relative error. However, the new data above 1000 K are lower than the corresponding drift tube results¹² for the reasons described below.

The SIFT and HTFA rate constants reflect thermal energy distribution of the reactants at the flow tube temperature, which covers the range from 300 to 1400 K for the current measurements. A survey of numerous past high temperature studies of the kinetics of ion-molecule reactions shows that having energy in either reactant translation or rotation usually affects the reactivity equally.^{1,30} To investigate the role of rotational and translational energy, particularly at high temperatures, the rate constants are alternatively plotted versus the sum of the average rotational and translational energy in Fig. 2. The average rotational energy of the NO is simply $k_B T$, where T is the reaction temperature, and the average kinetic energy in the SIFT and HTFA is simply

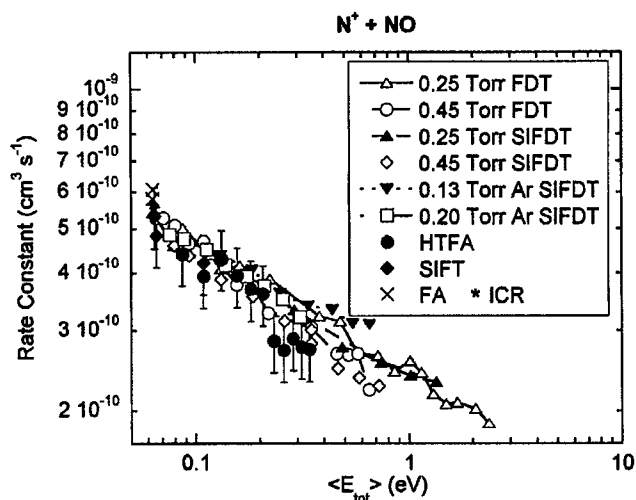


FIG. 3. Rate constants for the reaction of N^+ with NO plotted as a function of the average total energy (translational, rotational, and vibrational) in eV. The FDT and SIFT data are from Fahey *et al.* (Ref. 12). The HTFA data are current measurements. The SIFT data represent previous measurements at 298 K by Adams, Smith, and Paulson (Ref. 18) and Tichy *et al.* (Ref. 17) as well as the current SIFT measurements at 300 and 500 K. The FA value is from Matsuoka *et al.* (Ref. 26) and the ICR value is from Anicich, Huntress, and Futrell (Ref. 16).

$3/2k_B T$. The new SIFT and HTFA data are in excellent agreement with the drift tube data¹² up to 0.2 eV. However, the HTFA data above 0.2 eV are slightly lower than the drift tube values.¹² Nevertheless, these data are in agreement within the experimental error when plotted against rotational and translational energy. This agreement indicates that rotational and translational energy influence the reactivity equally within the uncertainty of the measurements.

One of the advantages of the HTFA experiments is that excited vibrational levels are thermally populated at higher temperatures. The drift tube data have been taken at a flow tube temperature of 298 K; thus, the NO will have a room temperature internal energy distribution. The large vibrational energy spacing in NO prevents any significant thermal population of $v > 0$ at 298 K.³¹ Comparing the HTFA data measured at high temperatures with drift tube data plotted as a function of the total energy in the reactants (translational, rotational, vibrational, and electronic energy, the latter being less than 0.01 eV³²) can illustrate the effects of vibrational excitation on the kinetics, which has often been shown to enhance reactivity.^{1,30} The rate constants are plotted again in Fig. 3 as a function of the average total energy in the reactants. The agreement between the drift tube and the HTFA measurements in Fig. 3 is somewhat better than in Fig. 2, clearly agreeing within the experimental error. No substantial enhancement of the rate constants occurs with vibrational excitation of the NO. Therefore, all types of energy affect the reaction of N^+ with NO equally, although the conclusions about vibrational excitation are only approximate because of the small amount of vibrational excitation even at the highest temperature. Previous studies involving NO have also shown smaller effects due to NO vibrational excitation than many other molecules.^{1,33}

Kosmider and Hasted made a static drift tube (DT) measurement of the kinetic energy dependence of the rate con-

TABLE I. Product branching ratios for the reactions of N^+ and N_3^+ with NO measured in the selected ion flow tube (SIFT) at 300 and 500 K. The room temperature values have been taken from the literature as indicated in the table. The enthalpy of reaction at 298 K, $\Delta H_{rxn}^{298 K}$, has been calculated from the literature values (see text).

Reaction	$\Delta H_{rxn}^{298 K}$ kJ mol ⁻¹	Branching ratios		
		300 K	300 K Literature	500 K
$N^+ + NO \rightarrow O^+ + N_2$	-408	0.02	<0.05 ^a	0.01
$N_2^+ + O$	-212	0.07	0.08 ^b	0.11
			0.15 ^c	
			0.21 ^d	
$NO^+ + N$	-511	0.91	0.92 ^b	0.88
			0.85 ^c	
			0.79 ^d	
$N_3^+ + NO \rightarrow NO^+ + N_2 + N$	-212	1.00		1.00

^aFahey *et al.* (Ref. 12).

^bAnicich, Huntress, and Futrell (Ref. 16).

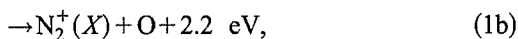
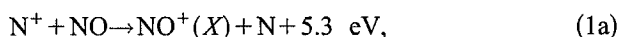
^cAdams, Smith, and Paulson (Ref. 18).

^dTichy *et al.* (Ref. 17).

stants for this reaction at energies between 0.04 and 2 eV.¹¹ While their data show some limited qualitative similarities to the flow tube data, their rate constants are an order of magnitude lower than all of the values taken by different methods discussed above. Consequently, these data have been omitted from Figs. 1–3. The authors noted several problems in determining the NO concentration in the drift tube. If the concentrations were erroneously high, the measured rate constants will appear lower than the actual values.

In addition, the cross sections for the reaction of N^+ with NO giving NO^+ and N_2^+ have been measured using a crossed beam apparatus to investigate the ion kinetic energy dependence.^{25,27} These data were converted to rate constants by Fahey *et al.* by multiplying the cross section by the average center-of-mass collision velocity of the reactants, and then added together to get a total rate constant for comparison with their drift tube data.¹² The crossed beam derived rate constants show an increase with increasing kinetic energy and are in disagreement with the drift tube rate constants below 2.5 eV. Fahey *et al.* carefully eliminated the possible causes of error in their measurements, including the neglect of the minor O^+ product channel in the crossed beam data, the role of metastable N^+ ions in the crossed beam experiment,²⁷ and the effect of deviations of the ion speed distribution in the flow drift tube from near Maxwellian.¹² As the data from the many different sets of experiments shown in Figs. 1–3 agree very well, these crossed beam results^{25,27} have also been excluded.

Branching ratios for this reaction at 300 and 500 K have been measured in the SIFT and are shown in Table I along with the literature values at 298 K. The data have been corrected for the presence of a <2% H_2O^+ impurity that persisted despite trapping the helium buffer as well as $\leq 3\%$ background impurities of N_2^+ , NO^+ , and O_2^+ from the reaction of N^+ with trace impurities in the buffer gas. The branching ratios previously measured at room temperature in a SIFT (Refs. 17, 18) and in an ICR (Ref. 18) are also shown in Table I. The three potential reaction channels are shown in Eq. (1) below.³¹



The predominant product observed in the SIFT is nondissociative charge transfer yielding NO^+ , accounting for 0.91 of the products at 300 K and 0.88 of the products at 500 K. The previous values are in the 0.79–0.93 range^{16–18} and the 300 K data are in closest agreement with the ICR value of Anicich, Huntress, and Futrell.¹⁶ The other major reaction channel gives products N_2^+ and O, where the N_2^+ branching fraction increases from 0.07 at 300 K to 0.11 at 500 K. This is outside our error of 20% of the minor channel. Again, the new 300 K value agrees best with the ICR result.¹⁶ Creating either the $N_2^+(A)$ or $O(^1D)$ excited neutral products is 1.1 and 0.21 eV exothermic, respectively. The relatively small amount of N_2^+ may indicate barriers along this reactive pathway or competition with charge transfer. Fahey *et al.* have also examined the possibility of forming O^+ and N_2 products at high kinetic energies and place an upper limit on the O^+ branching ratio of 0.05 from 0.05 to 1.5 eV.¹² The present values show a minor O^+ product with a branching fraction of 0.02 and 0.01 at 300 and 500 K, respectively, consistent with the earlier observations. The O^+ product can also be exothermically produced in the 2D electronic excited state.³²

Tichy *et al.* have found the highest fraction of N_2^+ products (0.21) in a SIFT experiment that probed the reactivity of both ground and excited state N^+ using monitor ion techniques.¹⁷ The reaction of N^{+*} with H_2 giving H_2^+ provides a measure of the reactivity attributable to the metastable ions present. However, the authors note that N^+ reaction with H_2 complicates the deconvolution of the quenching of N^{+*} relative to reaction. N^+ reacts rapidly with H_2 to give NH^+ which, in turn, reacts rapidly with NO to give N_2H^+ at $m/z=29$.¹⁸ If the product mass analyzer resolution is insufficient to resolve 1 amu, then the N_2^+ contribution may be artificially inflated in the Tichy *et al.* SIFT results. Adams *et al.* have measured a branching ratio of 0.15 for N_2^+ in a SIFT, twice the value obtained currently. Adams *et al.* have noted that the source conditions have been carefully established to minimize the production of metastable N^+ ions so the presence of excited species should not interfere with their measurement. No obvious explanation can be found for the discrepancies between the current and previous results. All of the N_m^+ ions are present in the HTFA during these measurements, precluding the measurement of branching ratios.

B. $N_2^+ + NO$

The reaction of N_2^+ with NO has also been extensively studied by various methods.^{10,13,14,17,23–26,34–43} The rate constants for this reaction are plotted as a function of temperature in Fig. 4. Again, the data follow a power law dependence, $k=(7.5 \times 10^{-9})T^{-0.52}$. The dependence of the rate constant for $N_2^+(v=0)$ on the center-of-mass kinetic energy $\langle KE_{c.m.} \rangle$ has been measured in two separate SIFDT experiments using a monitor gas to isolate the N_2^+ ground vibra-

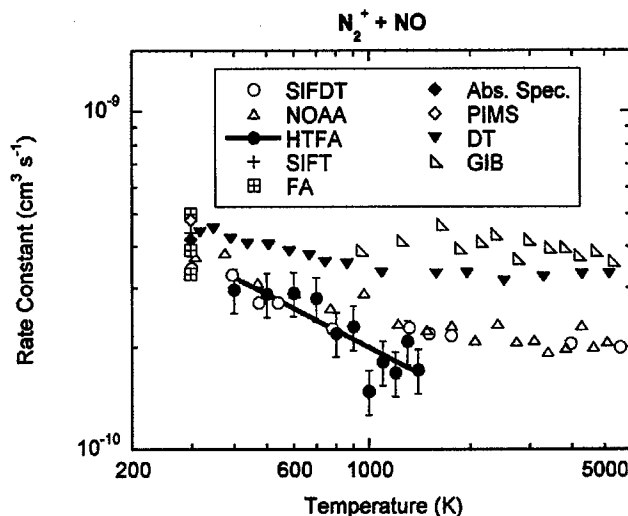


FIG. 4. Rate constants for the reaction of N_2^+ with NO plotted as a function of temperature in K. The SIFDT data sets are from Dobler *et al.* (Ref. 13) (labeled SIFDT) and Howorka, Albritton, and Fehsenfeld (Ref. 14) (labeled NOAA). The HTFA data are current measurements. The SIFT data represent previous measurements by Tichy *et al.* (Ref. 17) and Frost *et al.* (Ref. 43). The FA values are from Matsuoka *et al.* (Ref. 26), Goldan *et al.* (Ref. 23) and Fehsenfeld *et al.* (Ref. 24). The kinetic absorption spectrum result is from Dreyer and Perner and the photoionization mass spectrometry (PIMS) value is from Warneck (Ref. 16). The drift tube (DT) data are from Kobayashi and Koneko (Ref. 10) and the guided ion beam (GIB) data are from Graul *et al.* (Ref. 42).

tional state kinetics. For clarity, the Innsbruck SIFDT results of Dobler *et al.*¹³ are labeled SIFDT and the SIFDT results of Howorka, Albritton, and Fehsenfeld¹⁴ measured at NOAA are labeled NOAA in Fig. 4 and subsequent figures. Cross sections for this reaction as a function of $\langle KE_{c.m.} \rangle$ measured in a static DT by Kobayashi and Koneko¹⁰ and in a guided-ion beam (GIB) by Graul *et al.*⁴² have been converted to rate constants by taking the product of the cross section and the average relative velocity of the reactants in the center of mass. All of the $\langle KE_{c.m.} \rangle$ from the previous experiments^{10,13,14,42} have been converted to an effective temperature as described above for N^+ . An additional crossed beam experiment by Turner, Rutherford, and Stebbings has probed the cross sections as a function of kinetic energy for this reaction.²⁵ However, their measurements have been made at kinetic energies of 4 eV and higher, which exceeds the overlapping range of the experiments shown in Fig. 4 and have consequently not been shown.

The rate constant at 298 K for N_2^+ reacting with NO is well established at around $4.0 \pm 1.0 \times 10^{-10} \text{ cm}^3 \text{ s}^{-1}$.^{10,13,14,17,23,24,26,34–38,43} Again, this average value is roughly half of the Su-Chesnavich collision rate constant^{28,29} of $8.5 \times 10^{-10} \text{ cm}^3 \text{ s}^{-1}$. The current HTFA results agree with the previous studies showing that the rate constants decrease with increasing temperature. The two SIFDT studies^{13,14} agree very well with the HTFA data up to 900 K. The HTFA rate constant measured at 1000 K appears out of line with the other values. Varying the HTFA reaction conditions including filament emission current, N_2 source gas flow, sampling voltage, detector voltages, lens conditions, and electron energy did not affect the rate constant at 1000 K, eliminating the most commonly found sources of

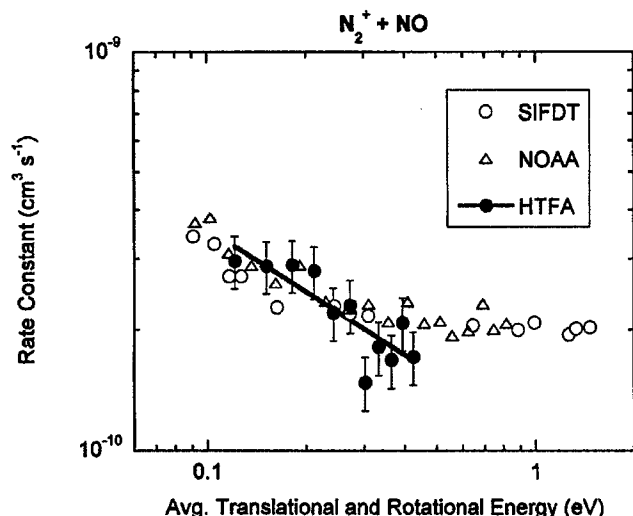


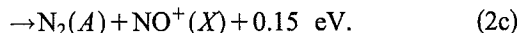
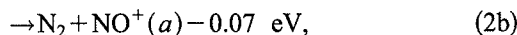
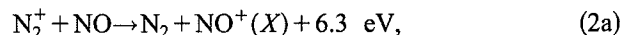
FIG. 5. Rate constants for the reaction of N_2^+ with NO as a function of the average translational and rotational energy in eV. The selected ion flow drift tube data sets are from Dobler *et al.* (Ref. 13) (labeled SIFT) and Horwoka, Albritton, and Fehsenfeld (Ref. 14) (labeled NOAA). The HTFA data are current measurements. The SIFT data represent previous measurements by Tichy *et al.* (Ref. 17) and Frost *et al.* (Ref. 43). The FA values are from Matsuoka *et al.* (Ref. 26), Goldan *et al.* (Ref. 23), and Fehsenfeld, Schmelt-ekopf, and Ferguson (Ref. 24). The kinetic absorption spectrum result is from Dreyer and Perner and the PIMS value is from Warneck (Ref. 16). The DT data are from Kobayashi and Koneko (Ref. 10) and the GIB data are from Graul *et al.* (Ref. 42).

error. In spite of these tests, we believe the shape of the data curve indicates that there must be a small systematic error in that point. The DT data agree with the flow tube results at 298 K and both the GIB and DT data exhibit the same qualitative trend. However, the DT and GIB data are systematically higher. We have no obvious explanation for the discrepancy. However, our past experience has proven that data obtained with the HTFA and obtained with the NOAA and Innsbruck drift tubes are generally in excellent agreement. Therefore, in order to derive internal energy dependences, we compare the HTFA results only to the SIFT and NOAA data.

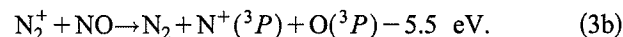
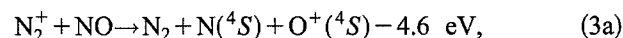
To investigate the role of translational and rotational energy at increased temperatures, the rate constants are also plotted against the average translational and rotational energy in Fig. 5. Only the HTFA, SIFT and NOAA data are plotted for clarity. The average rotational energy for NO in all of the experiments is $k_B T$, where T is the temperature of the experiment. The average rotational energy in the N_2^+ in the drift tube experiments^{10,13,14} is $k_B T_{\text{buf}}$, where T_{buf} is determined from the center-of-mass collision energy for ion-buffer gas collisions ($\langle KE_{\text{buffer}} \rangle = 3/2 k_B T_{\text{buf}}$).⁴⁴ The HTFA, SIFT (Ref. 13), and NOAA¹⁴ data sets in Fig. 5 agree within the error in the experiments, intimating that translational and rotational energy behave similarly. The HTFA data are lower than the drift tube data at temperatures over 1000 K but just at the limit of our uncertainty estimate. This discrepancy could be due to vibrational excitation reducing the reaction rate. However, it would mean that the $v > 0$ rate constants would be effectively zero and therefore, the difference is more likely a result of a small systematic error in one of the measurements. In any case, it is clear that vibrational

excitation does not significantly enhance the rate constants. For N_2^+ vibrations, it is shown that the rate constant for reactivity is similar between various states and that the overall rate constant increases because of quenching.^{13,14}

The reaction of N_2^+ with NO proceeds almost exclusively via charge exchange to give NO^+ . Three energetically possible channels are illustrated below in Eq. (2).³¹



At collision energies above 5 eV in the GIB, two dissociative charge transfer channels giving N^+ and O^+ have been observed when these pathways become energetically accessible as shown in Eq. (3).⁴²



Production of the $NO^+(a)$ in the HTFA experiments could cause the apparent rate constants for reaction (2) to be slightly smaller since the $NO^+(a)$ ions would charge transfer back to N_2^+ .⁴⁵ However, no curvature in the HTFA data indicative of this back reaction has been observed, nor do the rate constants depend on the N_2 flow rate. As discussed previously, product branching ratios could not be obtained in the HTFA because all three of the N_m^+ ions are present under the current experimental conditions.

As previously mentioned, around 10% of the N_2^+ vibrational population is in $v=1$ at 1400 K. The quenching of vibrationally excited N_2^+ by NO in competition with the charge transfer reaction has been studied previously.^{13,14,17,38,40,41,43} Most recently, Frost *et al.*⁴³ have used a SIFT with laser-induced fluorescence detection of the N_2^+ vibrational levels to probe the competing processes. As found previously,⁴¹ the $v=1$ levels decay at a faster rate than $v=0$. However, ca. 70% of the reaction from $v=1$ is charge transfer giving NO^+ with a rate constant only 10% larger than that for $v=0$.⁴³ The HTFA results show that all types of energy affect the energy essentially the same, in keeping with the results of Frost *et al.*⁴³

C. $N_3^+ + NO$

Unlike N^+ and N_2^+ , only one previous study of the rate constant for the reaction of N_3^+ with NO has been performed.¹⁵ Lindinger has studied the kinetic energy dependence of the rate constant in a FDT at two different flow tube pressures at 298 K using a nitrogen buffer. The rate constants as a function of temperature are plotted in Fig. 6, where the $\langle KE_{c.m.} \rangle$ from the FDT is converted to T_{eff} as discussed above. All of the data sets shown in Fig. 7 agree well, except at 500 K where the SIFT value is slightly lower than the FDT results. However, the rate constants agree within the combined error of the two experiments. The rate constants are much less than the Su-Chesnavich collision rate constant^{28,29} of $7.7 \times 10^{-10} \text{ cm}^3 \text{ s}^{-1}$. Nevertheless, given the excellent agreement as a function of temperature between the FDT and HTFA, the data can be compared as a function of total en-

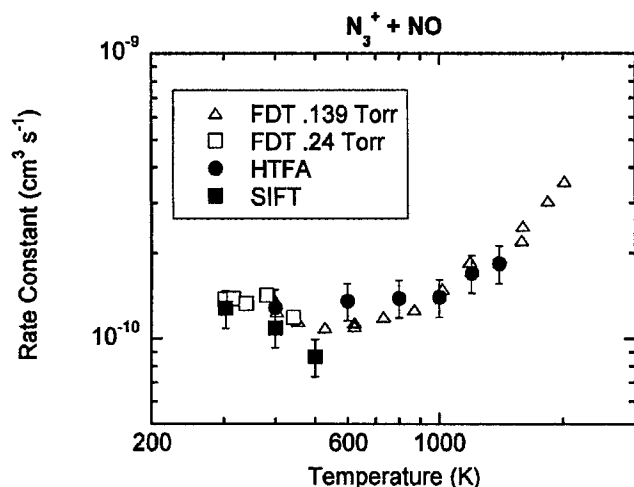


FIG. 6. Rate constants for the reaction of N_3^+ with NO plotted as a function of temperature in K. The flow drift tube (FDT) data are from Lindinger (Ref. 15). The SIFT and the HTFA data are current measurements.

ergy as shown in Fig. 7 to examine the role of the total energy available. The translational, rotational, and vibrational energy in N_3^+ and NO are calculated similarly as for the N_2^+ reaction. An important difference is that the vibrational temperature of the N_3^+ in the FDT reflects T_{buf} . When plotted this way, the HTFA data in Fig. 7 are lower than the FDT data at energies above 0.4 eV; however, the rate constants still agree within the error of the two experiments. One major difference is that the FDT experiments have been done in an N_2 buffer.¹⁵ Therefore, the ion velocity distribution will be different from similar measurements in a helium buffer and the remaining differences may be attributable to the difference in the energy distribution using N_2 as the buffer gas in the drift tube.⁴⁶

Lindinger¹⁵ proposes that N_2O^+ products may be formed exothermically in the N_3^+ reaction.³¹ However, only nondissociative charge transfer giving NO^+ has been observed in the SIFT at 300 and 500 K as shown in Table I and

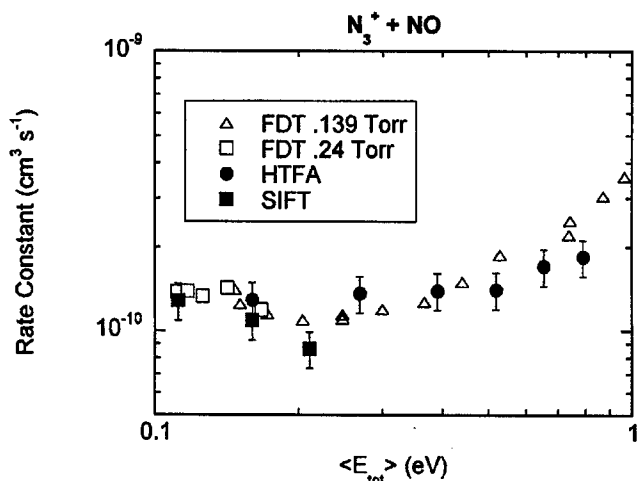


FIG. 7. Rate constants for the reaction of N_3^+ with NO plotted as a function of the average total energy (translational, rotational, and vibrational) in eV. The FDT data are from Lindinger (Ref. 15). The SIFT and the HTFA data are current measurements.

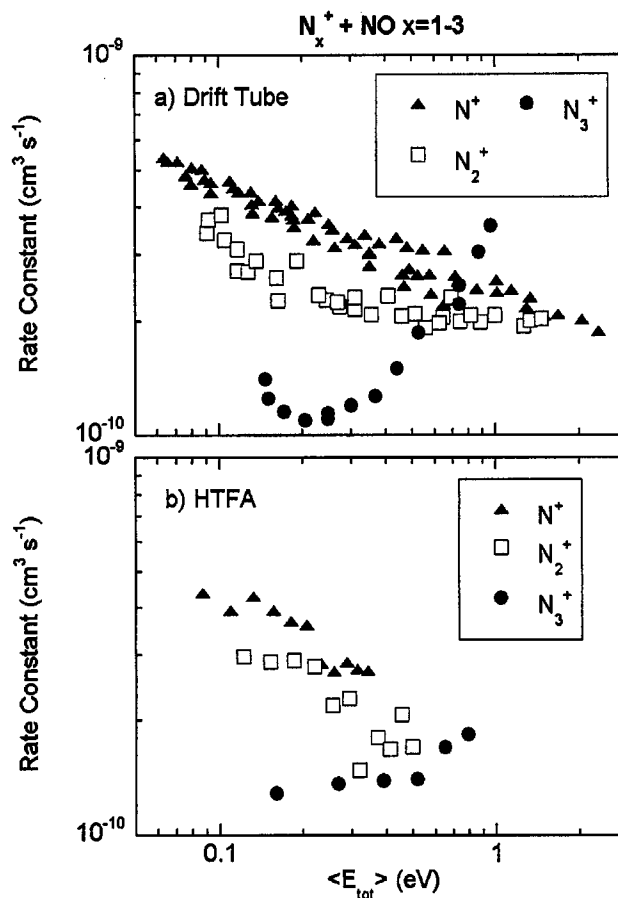
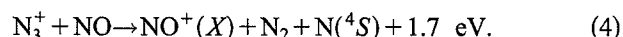


FIG. 8. Rate constants for the reactions of N^+ , N_2^+ , and N_3^+ with NO as measured using (a) drift tube instruments [N^+ (Ref. 12), N_2^+ (Refs. 13,14), and N_3^+ (Ref. 15)] and (b) a HTFA.

illustrated in Eq. (4) below. The heat of formation of N_3^+ used to calculate the reaction enthalpy is an average of data taken from the literature,^{31,47-49}



Forming linear N_3 products intact instead of dissociated as shown above is also exothermic;^{31,47-49} however N_3 is unstable. The branching ratios have not been measured previously¹⁵ and are unable to be examined in the HTFA for reasons outlined above.

IV. DISCUSSION

Figure 8 shows all of the energy dependent kinetics data measured using flow tubes for $N_m^+ + NO$ with $m = 1-3$ plotted together versus the average total energy available. All of the drift tube data are plotted in the top graph and all of the HTFA data are in the bottom graph. The overall rate constant for a given ion decreases with an increasing number of N atoms in the cation. However, the $N_3^+ + NO$ rate constants show a marked increase with increasing energy above ca. 0.25 eV in both the drift tube and the HTFA. The Franck-Condon factors at the charge transfer energy resonance with NO based on the recombination energies³¹ of the reactant ions for N^+ (14.53 eV), N_2^+ (15.58 eV), and N_3^+ (11.27 eV) producing the $NO^+(X)$ state are not favorable for any of the

ions.^{50,51} The mechanisms below are complicated and several mechanisms may play a role which may account for variations in the reactivity as seen in Fig. 8.

The trends in the rate constants with energy are indicative of reactions involving a collision complex. N^+ reacting with NO could form an N_2O^+ intermediate. It is 6.6 eV exothermic to form N_2O^+ in its linear ground electronic state in this manner.³¹ If ~ 5 eV or more of the exothermicity is in electronic energy of the intermediate, dissociation of linear N_2O^+ can occur from the $B^2\Pi$ electronic excited state.^{52,53} TPEPICO experiments of Nenner *et al.* have shown that this state is predissociative, giving $>99\%$ NO^+ and N_2^+ ,⁵⁴ consistent with the SIFT data from 298 to 500 K. NO^+ products can also be produced via predissociation from (1) the weakly spin-orbit coupled linear $N_2O^+A^2\Sigma$ first excited electronic state to either the $2^4\Sigma^-$ state^{53,55,56} or $1^4\Pi$ state,⁵³ (2) from the linear $N_2O^+X^2\Pi$ ground state to the $2^4\Sigma^-$ state,^{53,55,56} or (3) from the lower lying bent $N_2O^+a^4A''$ state that is correlated to the $^4\Pi$ linear excited state.^{52,57} The minor O^+ channel is only accessible from predissociation of the linear $N_2O^+X^2\Pi$ ground state to the $2^4\Sigma^-$ state^{53,55} or from access to the bent a^4A'' state.^{52,57} The bent configuration has a small energy barrier (~ 0.1 eV) to ground state $O^+ + N_2$ products. However, the shape of the saddle point region creates a dynamical barrier that affects the reaction probability.^{52,57}

A more direct mechanism may contribute to the $N^+ + NO$ reaction as well. The strongest Franck-Condon overlap would be at the resonance with the $NO^+(X) + N(^2P)$ products, where the product curve crosses at around $NO(v=4)$, but this crossing would form a large barrier to charge exchange along this coordinate. It is possible that the entrance channel potential could shift relative to the product potential as the reactants approach each other. This region of the potential would be controlled by the global minimum of the N_2O^+ surface instead, possibly creating resonances with the off-resonant $NO^+(X, v=4,5)$ levels which have sufficient Franck-Condon overlap. The asymptotic Franck-Condon factors may also be different at shorter ranges.⁵⁸

For the N_2^+ reaction with NO, Graul *et al.* have found from time-of-flight (TOF) product velocity distribution measurements that two charge transfer mechanisms occur: formation of a collision complex involving ion-induced dipole forces and a direct charge transfer controlled by energy resonance and Franck-Condon factors with large internal energy deposition, even at collision energies below 1 eV.⁴² The $NO^+(a)$ excited electronic state shown in Eq. (2b) is nearly resonant and has good Franck-Condon overlap with $NO(X, v=0)$ and could easily participate in a direct mechanism.^{50,51} However, the TOF spectra are not sufficiently resolved to indicate whether the electronically excited products are from channels (2b) or (2c).⁴²

The cross sections for the forward scattered NO^+ products observed in the TOF spectra in the GIB for $N_2^+ + NO$ have an $E^{-0.5}$ center-of-mass translational energy dependence, indicative of creating an orbiting collision complex at kinetic energies below 1 eV.⁴² A power law fit to the HTFA data also gives an $ca. E^{-0.5}$ energy dependence, consistent with the observations of Graul *et al.*⁴² Parent *et al.*³⁹

have found through measuring product kinetic energy distributions using an ICR that significant product translational energy occurs, consistent with more of the complex formation mechanism contributing at thermal energies than at 1 eV and higher in the GIB. The internal energy appears to be deposited in the excited vibrational levels of ground electronic state products and likely some of the energy is also deposited in the $N_2(A, v=0)$ state. However, no evidence for generating ground electronic state products is observed above 1 eV in the GIB.⁴²

Triplet N_3^+ reacting with doublet NO can react via a collision complex accessing either a doublet or quartet surface to produce NO^+ . Forming ground state linear N_3 via this reaction is 1.9 eV exothermic. However, the doublet ground state linear N_3 is unstable relative to dissociation forming the spin-forbidden ground state products $N(^4S^0) + N_2$ and it is 2.3 eV below the spin-allowed $N(^2D) + N_2$ asymptote.^{48,59} Recent calculations of the potential energy surface for the dissociation of N_3 by Zhang *et al.* using multireference configuration interaction (MRCI) at the MR-CISD(Q) level using a triple-zeta basis set (VTZ) show that a crossing seam accessing the quartet surface leading to $N(^4S^0) + N_2$ is around 2 eV above the doublet linear N_3 ground state.⁵⁹ This seam is accessible if linear N_3 is formed in reaction (4) with most or all of the 1.9 eV exothermicity deposited into N_3 internal energy. Therefore, the neutral products are most likely $N(^4S^0) + N_2$ which is overall 1.7 eV exothermic. Alternatively, the lowest stable doublet N_3 excited state is a cyclic isomer *ca.* 1.3 eV higher in energy. However, a ~ 1.2 eV barrier to isomerization exists from the linear ground state, making this pathway less likely over the energy range presently studied.⁶⁰ In addition, the potential surfaces explicitly for the $N_3^+ + NO$ system are unknown. Thus, the topology of the surface for the N_3^+ reaction may be the reason that its behavior is so different from that of N^+ and N_2^+ .

V. CONCLUSIONS

This work continues our series of studies on how different forms of energy affect the rate constants for ion-molecule reactions. Previously, we have shown that in almost all cases, rotational and translational energy affect the reactivity equally within our error. All three reactions studied here confirm that observation. The effects of vibrational energy have been more varied. We have previously concluded that for charge transfer reactions, the effects of vibrations are often the same for reactions involving the same neutral reactant. This was certainly true for O_2 reactions, where O_2 vibrational excitation enhanced the reactivity.^{30,61–63} However, for NO reactions, only two have been studied up to 1400 K and no appreciable effect of vibrationally exciting NO was observed.^{64,65} All three reactions studied here are consistent with this observation. However, the large vibrational constant for NO results in only a small amount of excited NO, making accurate determination of the vibrational rate constants impossible. In any case, those rate constants cannot be appreciably larger than the ground state rate constant and are probably very similar. This conclusion is consistent with the Franck-Condon factors being large if the lowest $NO^+(X)$

vibrational levels are populated.^{50,51} All of the reactions with NO studied here involve a collision complex, consistent with the fact that redistribution of energy results in all forms of energy behaving the same. Curve crossings in the potential energy surface at long range for the systems involving NO may also have an influence on the observed reactivity.⁵⁸

The temperature dependence of the branching ratios for the N^+ reaction with NO has also been measured for the first time up to 500 K. An increase in the amount of N_2^+ products at the expense of NO^+ nondissociative charge transfer products occurs at 500 K. A small amount of O^+ product is also observed. The branching ratios for the reaction of N_3^+ with NO have also been measured in the SIFT, showing that only nondissociative charge transfer to give NO^+ occurs up to 500 K.

ACKNOWLEDGMENTS

The authors would like to thank Skip Williams, Yu-Hui Chiu, and Rainer Dressler for helpful discussions. They would also like to thank John Williamson and Paul Mundis for technical support. The work has been supported under Air Force Office of Scientific Research Project No. 2303EP4. A.J.M. and T.M.M. are under contract to Visidyne, Inc. of Burlington, MA through Contract No. F19628-99-C-0069.

- ¹ A. A. Viggiano and S. Williams, in *Advances in Gas Phase Ion Chemistry*, edited by N. G. Adams and L. M. Babcock (Academic Press, New York, 2001), Vol. 4, pp. 85–136.
- ² S. Williams, P. M. Bench, A. J. Midey, S. T. Arnold, A. A. Viggiano, R. A. Morris, L. Q. Maurice and C. D. Carter, in *JANNAF, 25th Airbreathing Propulsion Meeting* (Monterey, CA, 2000), Vol. 1, pp. 205–213.
- ³ S. Williams, A. J. Midey, S. T. Arnold, *et al.*, “Progress on the investigation of the effects of ionization on hydrocarbon/air combustion chemistry: kinetics and thermodynamics of C6-C10 hydrocarbon ions,” AIAA 2001–2873, 2001.
- ⁴ A. A. Viggiano and F. Arnold, in *Atmospheric Electrodynamics*, edited by H. Volland (CRC, Boca Raton, 1995), Vol. 1, pp. 1–25.
- ⁵ *Handbook of Geophysics and the Space Environment*, edited by A. S. Jursa (National Technical Information Service, Springfield VA, 1985).
- ⁶ D. Smith and P. Spanel, *Mass Spectrom. Rev.* **14**, 255 (1995).
- ⁷ T. C. Wei, L. R. Collins, and J. Phillips, *J. Phys. D* **28**, 295 (1995).
- ⁸ H. Hwang, J. K. Olthoff, R. J. Van Brunt, S. B. Radovanov, and M. J. Kushner, *J. Appl. Phys.* **79**, 93 (1996).
- ⁹ J. Levaton, J. Amorim, A. R. Souza, D. Franco, and A. Ricard, *J. Phys. D* **35**, 689 (2002).
- ¹⁰ N. Kobayashi and Y. Kaneko, *J. Phys. Soc. Jpn.* **37**, 1082 (1974).
- ¹¹ R. G. Kosmider and J. B. Hasted, *J. Phys. B* **8**, 273 (1975).
- ¹² D. W. Fahey, I. Dotan, F. C. Fehsenfeld, D. L. Albritton, and L. A. Viehland, *J. Chem. Phys.* **74**, 3320 (1981).
- ¹³ W. Dobler, H. Ramler, H. Villinger, F. Howorka, and W. Lindinger, *Chem. Phys. Lett.* **97**, 553 (1983).
- ¹⁴ F. Howorka, D. L. Albritton, and F. C. Fehsenfeld, 1980.
- ¹⁵ W. Lindinger, *J. Chem. Phys.* **64**, 3720 (1976).
- ¹⁶ V. G. Anicich, W. T. Huntress, Jr., and J. H. Futrell, *Chem. Phys. Lett.* **47**, 488 (1977).
- ¹⁷ M. Tichy, A. B. Rakshit, D. G. Lister, N. D. Twiddy, N. G. Adams, and D. Smith, *Int. J. Mass Spectrom. Ion Phys.* **29**, 231 (1979).
- ¹⁸ N. G. Adams, D. Smith, and J. F. Paulson, *J. Chem. Phys.* **72**, 288 (1980).
- ¹⁹ A. A. Viggiano, R. A. Morris, F. Dale, J. F. Paulson, K. Giles, D. Smith, and T. Su, *J. Chem. Phys.* **93**, 1149 (1990).
- ²⁰ P. M. Hierl, J. F. Friedman, T. M. Miller *et al.*, *Rev. Sci. Instrum.* **67**, 2142 (1996).
- ²¹ A. J. Midey, S. Williams, S. T. Arnold, and A. A. Viggiano, *J. Phys. Chem. A* **106**, 11726 (2002).
- ²² S. T. Arnold, S. Williams, I. Dotan, A. J. Midey, R. A. Morris, and A. A. Viggiano, *J. Phys. Chem. A* **103**, 8421 (1999).
- ²³ P. D. Goldan, A. L. Schmeltekopf, F. C. Fehsenfeld, H. I. Schiff, and E. E. Ferguson, *J. Chem. Phys.* **44**, 4095 (1966).
- ²⁴ F. C. Fehsenfeld, A. L. Schmeltekopf, and E. E. Ferguson, *J. Chem. Phys.* **46**, 2019 (1967).
- ²⁵ B. R. Turner, J. A. Rutherford, and R. F. Stebbings, *J. Geophys. Res.* **71**, 4521 (1966).
- ²⁶ S. Matsuoka, H. Nakamura, T. Fujii, and T. Tamura, *Mass Spectrosc. (Tokyo)* **32**, 253 (1984).
- ²⁷ J. A. Rutherford and D. A. Vroom, *J. Chem. Phys.* **64**, 1251 (1976).
- ²⁸ T. Su and W. J. Chesnavich, *J. Chem. Phys.* **76**, 5183 (1982).
- ²⁹ T. Su, *J. Chem. Phys.* **89**, 5355 (1988).
- ³⁰ A. A. Viggiano, W. B. Knighton, S. Williams, S. T. Arnold, A. J. Midey, and I. Dotan, *Int. J. Mass. Spectrom.* **223–224**, 397 (2003).
- ³¹ S. G. Lias, J. E. Bartmess, J. F. Liebman, J. L. Holmes, R. D. Levin, and W. G. Mallard, in *NIST Chemistry WebBook, NIST Standard Reference Database Number 69*, edited by W. G. Mallard and P. J. Linstrom (NIST, Gaithersburg, 1998); (<http://webbook.nist.gov>).
- ³² A. A. Radzig and B. M. Smirnov, in *Reference Data on Atoms, Molecules, and Ions*, edited by J. P. Toennies (Springer-Verlag, Berlin, 1985), Vol. 31, pp. 259–260.
- ³³ A. A. Viggiano and R. A. Morris, *J. Phys. Chem.* **100**, 19227 (1996).
- ³⁴ P. Warneck, *J. Geophys. Res.* **72**, 1651 (1967).
- ³⁵ F. C. Fehsenfeld, D. B. Dunkin, and E. E. Ferguson, *Planet. Space Sci.* **18**, 1267 (1970).
- ³⁶ J. W. Dreyer and D. Perner, *Chem. Phys. Lett.* **12**, 299 (1971).
- ³⁷ M. A. French, L. P. Hills, and P. Kebarle, *Can. J. Chem.* **51**, 456 (1973).
- ³⁸ W. Dobler, H. Villinger, F. Howorka, and W. Lindinger, *Int. J. Mass Spectrom. Ion Phys.* **47**, 171 (1983).
- ³⁹ D. C. Parent, R. Dera, G. Mauclair, M. Heninger, R. Marx, M. E. Rincon, A. O’Keefe, and M. T. Bowers, *Chem. Phys. Lett.* **117**, 127 (1985).
- ⁴⁰ E. E. Ferguson, *J. Phys. Chem.* **90**, 731 (1986).
- ⁴¹ E. E. Ferguson, R. Richter, and W. Lindinger, *J. Chem. Phys.* **89**, 1445 (1988).
- ⁴² S. T. Graul, S. Williams, R. A. Dressler, R. H. Salter, and E. Murad, *J. Chem. Phys.* **100**, 7348 (1994).
- ⁴³ M. J. Frost, S. Kato, V. M. Bierbaum, and S. R. Leone, *Chem. Phys.* **231**, 145 (1998).
- ⁴⁴ D. Smith and N. G. Adams, in *Gas Phase Ion Chemistry*, edited by M. T. Bowers (Academic, New York, 1979), Vol. 1, p. 1.
- ⁴⁵ I. Dotan, F. C. Fehsenfeld, and D. L. Albritton, *J. Chem. Phys.* **71**, 3280 (1979).
- ⁴⁶ D. L. Albritton, I. Dotan, W. Lindinger, M. McFarland, J. Tellinghuisen, and F. C. Fehsenfeld, *J. Chem. Phys.* **66**, 410 (1977).
- ⁴⁷ J. M. L. Martin, J. P. Francois, and R. Gijbels, *J. Chem. Phys.* **93**, 4485 (1990).
- ⁴⁸ R. E. Continetti, D. R. Cyr, D. L. Osborn, D. J. Leahy, and D. M. Neumark, *J. Chem. Phys.* **99**, 2616 (1993).
- ⁴⁹ D. A. Dixon, D. Feller, K. O. Christe *et al.*, *J. Am. Chem. Soc.* **126**, 834 (2004).
- ⁵⁰ R. W. Field, *J. Mol. Spectrosc.* **47**, 194 (1973).
- ⁵¹ D. L. Albritton, A. L. Schmeltekopf, and R. N. Zare, *J. Chem. Phys.* **71**, 3271 (1979).
- ⁵² D. G. Hopper, *J. Am. Chem. Soc.* **100**, 1019 (1978).
- ⁵³ N. Komih, *J. Mol. Struct.: THEOCHEM* **306**, 313 (1994).
- ⁵⁴ I. Jenner, P.-M. Guyon, T. Baer, and T. R. Govers, *J. Chem. Phys.* **72**, 6587 (1980).
- ⁵⁵ M. Richard-Viard, O. Atabek, O. Dutuit, and P.-M. Guyon, *J. Chem. Phys.* **93**, 8881 (1990).
- ⁵⁶ J. A. Beswick and M. Horani, *Chem. Phys. Lett.* **78**, 4 (1981).
- ⁵⁷ D. G. Hopper, *J. Chem. Phys.* **76**, 1068 (1982).
- ⁵⁸ R. A. Dressler, D. J. Levandier, S. Williams, and E. Murad, *Comments At. Mol. Phys.* **34**, 43 (1998).
- ⁵⁹ P. Zhang, K. Morokuma, and A. M. Wodtke, *J. Chem. Phys.* (to be published).
- ⁶⁰ M. Bitterova, H. Ostmark, and T. Brinck, *J. Chem. Phys.* **116**, 9740 (2002).
- ⁶¹ P. M. Hierl, I. Dotan, J. V. Seeley, J. M. Van Doren, R. A. Morris, and A. A. Viggiano, *J. Chem. Phys.* **106**, 3540 (1997).
- ⁶² I. Dotan, P. M. Hierl, R. A. Morris, and A. A. Viggiano, *Int. J. Mass Spectrom. Ion Phys.* **167/168**, 223 (1997).
- ⁶³ A. J. Midey and A. A. Viggiano, *J. Chem. Phys.* **109**, 5257 (1998).
- ⁶⁴ I. Dotan and A. A. Viggiano, *J. Chem. Phys.* **110**, 4730 (1999).
- ⁶⁵ A. J. Midey and A. A. Viggiano, *J. Chem. Phys.* **110**, 10746 (1999).